

Numerical Research on the Influence of Interceptor Flaps on the Planing Hydrodynamic Performance

Numeričko istraživanje utjecaja zakrilaca krmnog praga na hidrodinamičke performanse glisanja

Samuel

Diponegoro University
Faculty of Engineering
Department of Naval Architecture
Indonesia
E-mail: samuel@ft.undip.ac.id

Serliana Yulianti

Diponegoro University
Faculty of Engineering
Department of Naval Architecture
Indonesia
E-mail: serlianayulianti@students.undip.ac.id

Parlindungan Manik*

Diponegoro University
Faculty of Engineering
Department of Naval Architecture
Indonesia
E-mail: parlindunganmanik@lecturer.undip.ac.id

Andi Trimulyono

Diponegoro University
Faculty of Engineering
Department of Naval Architecture
Indonesia
E-mail: anditrimulyono@lecturer.undip.ac.id

Ahmad Firdhaus

Diponegoro University
Faculty of Engineering
Department of Naval Architecture
Indonesia
E-mail: ahmadf@lecturer.undip.ac.id

Tuswan

Diponegoro University
Faculty of Engineering
Department of Naval Architecture
Indonesia
E-mail: tuswan@lecturer.undip.ac.id

Dian Purnama Sari

The National Research and
Innovation Agency
Jl. Hidrodinamika
Indonesia
E-mail: dian010@brin.go.id

DOI 10.17818/NM/2023/4.4

UDK 629.57:551.465.11

Preliminary communication / Prethodno priopćenje

Paper received / Rukopis primljen: 3. 12. 2022.

Paper accepted / Rukopis prihvaćen: 19. 5. 2023.



Abstract

The trim tab and interceptor have been utilized to optimize the running trim and motion control of planing boats at varying speeds in calm water. Increasing the height of the interceptor can create excessive drag and bow-down trim. The effectiveness of the interceptor can be increased by integrating it with a horizontal flap. This research focuses on the impact of the influence caused by interceptor flaps on the pressure distribution and fluid flows around the vessel. To simulate trim and sinkage measurement, the environment was modeled in the two-degree of freedom condition. Variation of integrated interceptor flaps has been analyzed with Finite Volume Method (FVM) based on RANS (Reynolds-Averaged Navier-Stokes) equation using overset mesh. The turbulent $K-\epsilon$ and VOF (Volume of Fluid) models are used to model the water and air phases. The grid convergence study is performed to establish the parallel solver's grid independence. To confirm the accuracy of the test in the bare hull condition, the numerical approach was tested experimentally. The result of drag, trim, and sinkage was calculated and it has been proved that the added flaps into interceptors are very useful in drag reduction and trim control. The percentage of interceptor height is directly proportional to the resulting lift force. Higher lift force can more effectively improve trim and reduce drag. Overall, this study shows an improvement in ship performance when using an interceptor and interceptor flap. One of the model configurations in the study has been shown to reduce drag by up to 33.3% at Froude number 1.45 when compared to ships without an interceptor.

Sažetak

Trim ploče i krmni prag koriste se za optimizaciju trima u plovidbi i kontrolu kretanja glisera pri različitim brzinama u mirnoj vodi. Povećanje visine praga može stvoriti prekomjeran otpor i trim pramca prema dolje. Učinkovitost praga može se povećati integracijom s vodoravnim zakrilcem. Ovo istraživanje usmjereno je na učinak utjecaja zakrilaca krmnog praga na raspodjelu tlaka i strujanje tekućine oko plovila. Za simulaciju mjerenja trima i urona, okolina je modelirana u uvjetima od dvaju stupnjeva slobode. Varijacije integriranih zakrilca krmnog praga analiziraju se metodom konačnih volumena (FVM) koja se temelji na RANS (Reynolds-Averaged Navier-Stokes) jednadžbi korištenjem konvergencijom mreže. Za modeliranje vodene i zračne faze koriste se modeli turbulentnog $K-\epsilon$ i VOF (volumni protok). Analiza konvergencije mreže provedena je kako bi se utvrdila neovisnost mreže paralelnog solvera. Kako bi se potvrdila točnost testa u stanju golog trupa, numerički pristup testira se eksperimentalno. Izračunat je rezultat otpora, trima i urona te je dokazano da su dodana zakrilca krmnog praga vrlo korisna u smanjenju otpora i kontroli trima. Postotak visine krmnog praga izravno je proporcionalan dobivenoj sili uzgona. Veća sila uzgona može učinkovitije poboljšati trim i smanjiti otpor. Općenito, ova studija pokazuje poboljšanje u performansama broda pri korištenju zakrilcem krmnog praga. Pokazalo se da jedna od konfiguracija modela smanjuje otpor do 33,3% pri Froudeovu broju 1,45 u usporedbi s brodovima bez krmnog praga.

KEY WORDS

Interceptor flap
numerical simulation
planning hull hydrodynamics

KLJUČNE RIJEČI

zakrilce krmnog praga
numerička simulacija
hidrodinamika trupa gliserskog plovila

* Corresponding author

1. INTRODUCTION / Uvod

Changes in speed significantly affect the performance of fast boats. Dynamic instability causes various negative impacts on boat safety. To address this issue, an automatic control policy often employs active actuators such as flaps and interceptors to maintain a pre-calculated 'optimal' dynamic trim angle for minimum drag. The interceptor is able to move vertically due to a system controlled by a hydraulic mechanical engine [1]. The interceptor can control the trim so that it can reduce the ship's drag with good flexibility. The effect of the layout and blade height of the interceptor was illustrated using numerical simulation [2]. The interceptor can reduce drag by as much as 57% at a Froude number of 0.87 near the chine position [3]. Mansoori and Fernandes proved that the interceptor was able to improve ship behavior by controlling the porpoising effect [4]. The interceptor can reduce resistance up to 15% for monohull vessels and 12% for catamaran vessels [5]. Unfortunately, by applied interceptor in high Froude number caused a decisive moment and increase total drag.

On the other hand, the interceptor has the disadvantage on producing excessive pressure, resulting in bow-down trim on the ship. These conditions have the potential to increase ship resistance and are dangerous for ship safety. In calm water, Mansoori and Fernandes investigated interceptors using the CFD method. The study explains that interceptors can cause negative trim at certain speeds [6]. Other studies also state that interceptors can create excessive pressure, causing bow-down trim [4].

The stern flap is a device that can reduce drag while reducing trim angle. The working principle of the stern flap is almost the same as the interceptor. A stern flap is a plate that extends at an angle from the transom to the ship's buttock plane. It modifies ship operating trim, reduces propulsion resistance, and improves maximum speed. Important stern flap design considerations include chord length, flap angle referred to the hull bottom, and flap span across the transom. The stern flap is believed to be able to control the trim and create the ideal pressure. Several studies on stern flaps have been carried out. The stern flap can reduce drag up to 5.53% using the CFD approach [7]. Five stern flap models were subjected to experimental studies to determine the optimal geometric characteristics. The most optimal design can reduce resistance by up to 8.2%. Experimental studies show stern flaps can reduce drag by up to 7.2% [8]. Research conducted by Ghadimi showed that the stern flap was able to reduce EHP in the propulsion system [9]. However, interceptors can reduce pitch and sinkage motions in calm water and regular head waves compared to the hull without an interceptor [10]. Another device called the bulbous bow was investigated with experimental and numerical results indicate that a decrease in the total resistance up to 7% [11].

Tsai and Hwang conducted an experimental study to analyze the performance of stern flaps, interceptors, and their combination in calm water conditions [12]. Other studies also compared interceptors, stern flaps, and their combination with numerical simulation methods [13]. It is assumed that the interceptor flap can be used with better effectiveness because the height of the interceptor can be controlled so that it can improve the wake formed. Changes in the dimensions of the flaps can affect the fluid flow around the stern. The combination of interceptor and stern flap can present a new phenomenon, so research on this subject continues to be developed. The properties of the fluid flow, wave pattern, and

pressure distribution for the interceptor flap combination with a 12-degree flap angle have not been recorded. It is essential to comprehend what occurs during the installation of an interceptor flap and how fluid flows near the interceptor flap at the transom. It directs the designers to enhance the conduct of boats with interceptor flap installations.

The development of science followed by computational technology has an impact on increasing research based on numerical simulations. The application of genetic algorithm used in ship design is the primary step [14]. The most commonly used CFD methods for planing hull are Finite Element Method (FEM), Finite Volume Method (FVM), and Boundary Element Method (BEM). Yousefi et al showed that the experimental method and CFD resulted in a fairly good accuracy in analyzing the ship's planing hull. Numerical simulations using the finite volume method are often used to predict hydrodynamic performance on planing hull ships [15]. Until now, the FVM method has become one of the most popular methods used in numerical simulations [16]. Research shows that FVM is the most widely used choice for predicting ship planing hull performance in terms of accuracy [17]. The results of the experimental analysis and CFD can be said to have conformity with each other by reviewing the pressure distribution, wave contour, and ship resistance coefficient [18] and also estimating the energy efficiency design index from the data of ship resistance [19]. The Reynolds-Averaged Navier-Stokes (RANS) formulation is a mathematical model for solving fluid flow equations. It was created to simulate turbulence's effects on fluid flows. Turbulence is a phenomenon in fluid flows that occurs when the flow becomes unpredictable. It is distinguished by small-scale, high-frequency fluctuations in flow variables such as velocity, pressure, and temperature. The RANS formulation averages out these fluctuations over time to obtain a time-averaged flow description. This time-averaged description can be used to predict flow mean behavior, such as mean velocity and pressure distribution.

The selection of ship speed and dimensions has nothing to do with developing the RANS formulation. However, when using the RANS formulation to simulate the flow around a ship, selecting an appropriate simulation speed and scale is critical. It is crucial to select a simulation that accurately captures the effects of the ship's size and speed on the flow behavior around it. This study uses a turbulence model with a standard k epsilon to describe turbulence in the flow.

The novelty of this research is to analyze the combination of interceptor and stern flap on the performance of ship planing hull. This study represents the results of CFD by comparing the drag, sinkage, and trim values of the experiment Park et al [20]. Validation is carried out by RANS configuration and solving turbulence problems based on ITTC recommendations [21]. This study combines interceptor and flap to achieve a broader speed range for reduced drag and practical trim optimization. Changes in the length of the flap to the length of the interceptor were observed to form a wave pattern at the stern of the ship.

2. METHODOLOGY DESCRIPTION / Opis metodologije

2.1. Research object / Predmet istraživanja

The main dimensions of the planing hull, interceptor, and stern flap can be seen in Table 1. Figure 1 shows the design of the Planing Hull and Interceptor Flap.

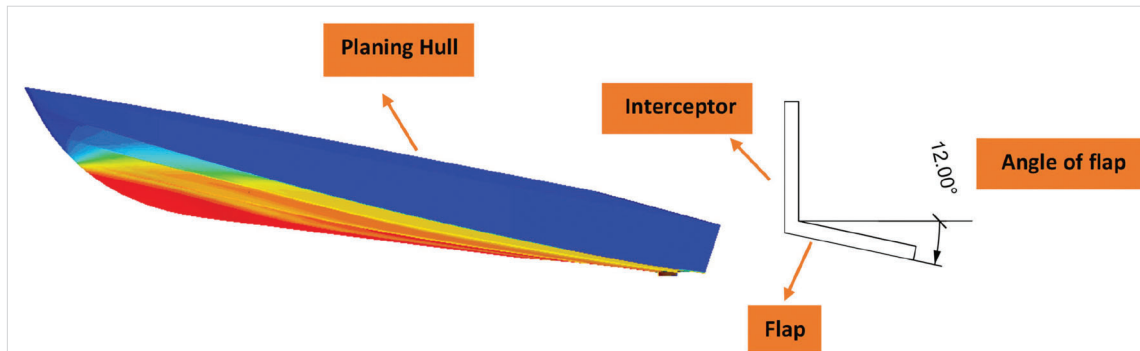


Figure 1 Design of planning hull and interceptor flap
Slika 1. Dizajn trupa gliserskog plovila i zakrilca krmenog praga

Table 1 Principal particulars of the planing hull
Tablica 1. Osnovni podaci glisirajućeg trupa

Main Particulars	Prototype	Model (scale 1:5.33)
Length overall, (m)	8	1.5
Length waterline, (m)	7.53	1.41
Breadth overall (m)	2.30	0.43
Draft (m)	0.44	0.08
Weight (Kg)	3.00	0.0019
Interceptor height, h_i (m)	5×10^{-5}	9.37×10^{-5}
Interceptor span, s (m)	0.30	56.25
Chine breadth (m)	2.20	0.41
C.G. from the transom, (m)	2.64	0.49
C.G. from baseline, (m)	0.76	0.14
Deadrise angle (°)	16 at the transom,	24 at midship

The dimensions of the modified interceptor flap can be seen in Table 2. This study uses the Aragon 2 ship which has been analyzed experimentally by Park et al [20]. Experimental testing refers to the commercial HUMPHREE X300 interceptor. The X300 interceptor is the initial design that will be tested using a numerical approach. The interceptor flaps were combined according to the comparison shown in Table 2.

Table 2 Combination of interceptor and stern flap
Tablica 2. Kombinacija krmenog praga i krmenog zakrilca

Variation	Interceptor	Stern Flap
interceptor	1d	-
S1	1/3 d	2/3 d
S2	2/3 d	1/3 d
S3	1/2 d	1/2 d
S4	1/4 d	3/4 d
S5	3/4 d	1/4 d

d = Interceptor or stern flap high

According to Mansoori and Fernandes' study, the angle of the stern flap used in each model was 120 degrees [22]. The combination configuration of the interceptor and stern flap in this study can be seen in Figure 2. The scale and size of the interceptor were selected based on experimental tests conducted by Park et al [20].

2.2. Solver settings / Postavke solvera

The discrete control volumes are created by dividing the domain into discrete grid volumes using the finite volume approach. The area between our geometrical margins is filled

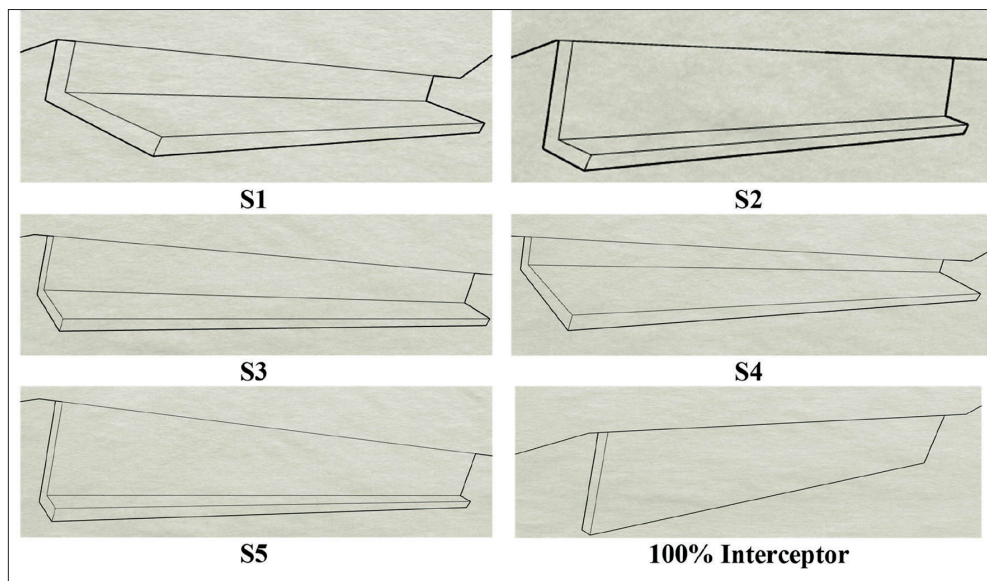


Figure 2 Design of interceptor flap
Slika 2. Dizajn zakrilca krmenog praga

by several nodes. The faces or boundaries of control volumes are positioned halfway between neighboring nodes. As a result, a control volume or cell encircles each node. It is customary to position control volumes close to the domain's boundary so that the physical boundaries and the control volume boundaries align. The grid should also have the ability to evaluate boundary layers, stagnation point regions, and separations. The calculation of the conservation of mass and momentum is carried out with the following formula [23]:

$$\frac{\partial(\rho)}{\partial t} + \frac{\partial}{\partial x_i}(\rho u_i) = 0$$

$$\frac{\partial(\rho u_i)}{\partial t} + \frac{\partial}{\partial x_j}(\rho u_i u_j) = -\frac{\partial p}{\partial x_j} + \frac{\partial}{\partial x_j} \mu \left(\frac{\partial u_i}{\partial x_j} - \overline{\rho u_i' u_j'} \right) + S_j \quad (1)$$

Where u_i and u_j were time-averaged values ($i, j = 1, 2, 3$) for the speed component; p was the time-averaged values of the pressure; ρ was the density; μ was the dynamic viscosity coefficient; $\overline{\rho u_i' u_j'}$ was the Reynolds stress term; S_j was the source term.

It is crucial to give the organized elements in the generated grid surrounding the body, particularly when there is a free surface in the simulation region, as the simulation of the free surface is highly dependent on the grid quality. To accurately imitate the waves, the grid surrounding the free surface must be of high quality. The number of elements is a crucial determinant in the quality of grid generation. The accuracy of numerical computation is created by high-quality mesh density, time step, and extra running time. Grid independence is used to prove that the mesh configuration is correct and that the mesh has no significant impact on the calculation results.

The output of this study is shear drag and pressure drag [24]. Shear drag is the tangential vector component of the total surface frictional resistance of the ship against fluids. While pressure drag is normal resistance or drags due to pressure which consists of wave and viscous pressure. Mathematically it can be formulated as follows:

$$f = \sum_f (f_f^{pressure} + f_f^{shear}) \cdot n_f \quad (2)$$

$$f_f^{pressure} = (P_f - P_{ref}) a_f \quad (3)$$

$$f_f^{shear} = -T_f \cdot a_f \quad (4)$$

Where:

P_f is static pressure

a_f is the area vector P_{ref} is normal pressure n_f is the node vector or fluid volume

T_f is the stress tensor.

This research referred to the Savitsky method to calculate lift force that influences the running state of planing hull, as follows [25]:

$$Cl = \frac{L}{0.5 \rho V^2 S} 10^3 \quad (5)$$

Where:

Cl is Lift coefficient

L is Lift force of the ship

ρ is fluid density

V is velocity of the ship

S is projected area of the plates on the free surface

$C_{L, interceptor}$ is the coefficient of lift force interceptor

$C_{L, flap}$ is the coefficient lift force flap

B is the breadth of the ship

l_{flap} is the lift force flap

$l_{interceptor}$ is the lift force interceptor

The increase in the lift force, drags, and trim with flap deflection is readily found by subtracting the force and moment for flap deflection. A hydrodynamic phenomenon known as the Stern Flap Effect occurs when a flap is attached to the aft end of a ship's hull. This flap covers a fixed area of the ship's surface and improves the vessel's performance. The lift force due to the flap is:

$$L_{flap} = 0.5 \rho V^2 L C_{flap} B C_{L, flap} \quad (6)$$

Where L_{flap} is the length of the chord of flap.

Furthermore, the interceptor lift coefficient is equal to:

$$C_{L, interceptor} = 0.046 \frac{L_{C, interceptor}}{B} \alpha_{interceptor} \quad (7)$$

$$L_{interceptor} = 0.5 C_{L, interceptor} \rho B^2 V^2 \quad (8)$$

Shear stress is the frictional force of the ship's surface against the fluid. In the case of a planing hull ship by reviewing the performance of fast boats including drag, sinkage, and trim, some of the ITTC recommendations followed in this study are:

1. The size of the computational domain
2. Mesh density
3. Convergence
4. Time step
5. Grid on the ship wall (y+)

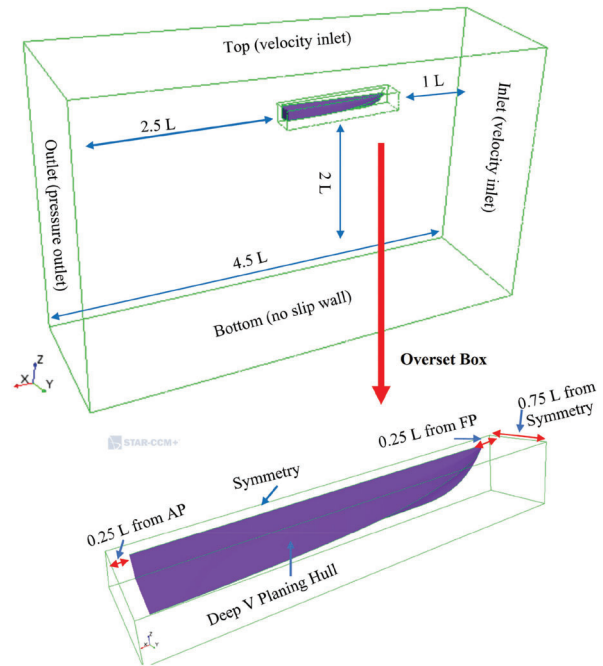


Figure 3 Computational domain and boundary condition
Slika 3. Računska domena i rubni uvjeti

Figure 3 shows the visualization of the boundary conditions and the computational domain. The computational domain and overset box dimensions use three-dimensional Cartesian coordinates. To reduce computation time, the symmetry plane is modeled to divide the ship along its longitudinal axis, and only a portion of the ship is analyzed. Boundary conditions are set as follows: Velocity inlet is present on top and side of the background. The outlet is on the aft side of the vessel and is defined as the pressure outlet. The bottom area describes a no-slip wall condition. The longitudinal area of the ship is called the symmetry plane. The symmetry boundary condition defines a mirror face/surface. It should only be used if the physical object

or geometry of the developed solution and the expected flow field pattern are mirrored along that surface. It indicates that no wave reflection will occur. To avoid the interaction between the reflected wave and the background domain. The fluid domain was discretized using a hexahedral unstructured mesh type with local refinements at the regions of special interest and where a more precise resolution of the flow was needed. The detail of refinement was shown in Figure 4.

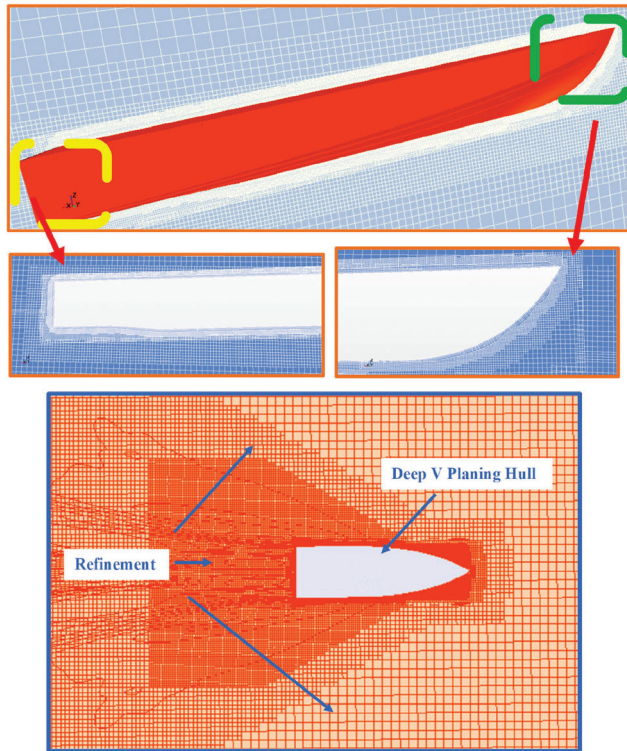


Figure 4 Mesh density
Slika 4. Gustoća mreže

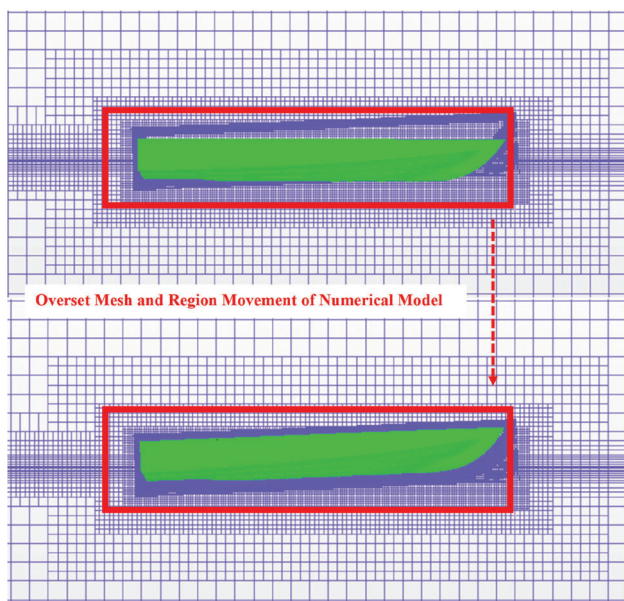


Figure 5 Overset mesh visualization
Slika 5. Vizualizacija konvergencije mreže

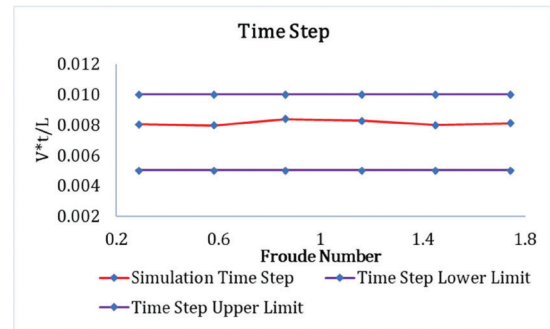


Figure 6 Time step
Slika 6. Vremenski korak

In a ship motion simulation, Dynamic Fluid Body Interaction (DFBI) is defined by presenting trim and sinkage (two degrees of freedom). The overset box is used as space for the ship's 2 DOF movement as shown in figure 5. Mathematically, the definition of ship motion is as follows [26]:

$$M\ddot{z} = \sum F_z \quad (9)$$

$$I\ddot{\theta} = \sum M_y \quad (10)$$

Where M is the mass and I is the moment of inertia of the ship.

The time step is defined by involving the CFL (Courant Fredrich Lewy) number which involves the flow velocity and the overall length of the ship as well as the complexity of the turbulence model. The time step used is in the range of 0.008 as described in Figure 6. Finer meshes with more minor elements typically produce more accurate results. Finer meshes, on the other hand, take longer to solve. However, there comes the point where the mesh is refined enough to capture the results accurately.

In CFD simulations, y^+ is a parameter used to determine the type of boundary layer near a solid surface. The y^+ wall function is used to predict the thickness of the first layer of the mesh near the wall, reducing results inaccuracy. y^+ is expressed in dimensionless units. ITTC recommends y^+ value of $30 < y^+ < 100$. Lotfi et al apply y^+ value of $50 < y^+ < 150$ for stepped planing vessels [27]. Avci et al suggest y^+ be in the range of 45-60 [28].

This study applies the range of y^+ value is 35-70, as shown in Figure 7. The prediction of friction on the bottom of the ship will be greatly influenced by the size of the y^+ value. Therefore, the study of the value of y^+ becomes one of the most important things to do to achieve the most suitable wall distance. The thickness of the prism layer is one of the techniques used to enhance the accuracy of boundary layer prediction on the ship's hull. The layer is equal to the thickness of the boundary layer, following the accuracy of the boundary layer, using the y^+ parameter. Referred by ITTC, the equations according to y^+ :

$$\Delta t = 0.005 \sim 0.01 L/U \quad (11)$$

Where: Δt : time step

L : Length of the ship

U : Speed of the ship

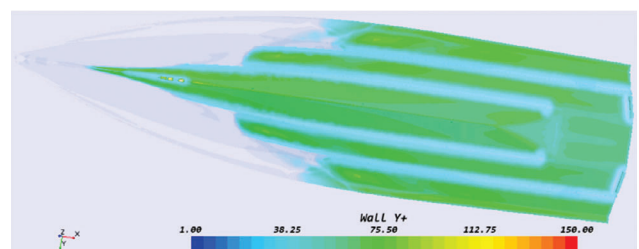


Figure 7 Wall y^+
Slika 7. Zid y^+

3. RESULTS AND DISCUSSION / Rezultati i rasprava

3.1. Grid independence study / Analiza neovisnosti mreže

This study uses five variations of the mesh quantity with a total of 0.52; 0.66; 0.87; 1.24 and 1.47 million cells. The grid study was conducted on Froude number 1.072. Figure 8 shows the results of the analysis of each grid independence study. The five variations of the grid have given a fairly good convergence

result. Grids 4 and 5 show the most accurate results compared to others. However, grid 5 takes a long time to complete one simulation. On the other hand, grid 4 has shown a very consistent value as well as a more economical time which can be observed in Figure 9. Therefore, this study uses a mesh number of 1.24 million cells for each simulation in terms of verification and research variation.

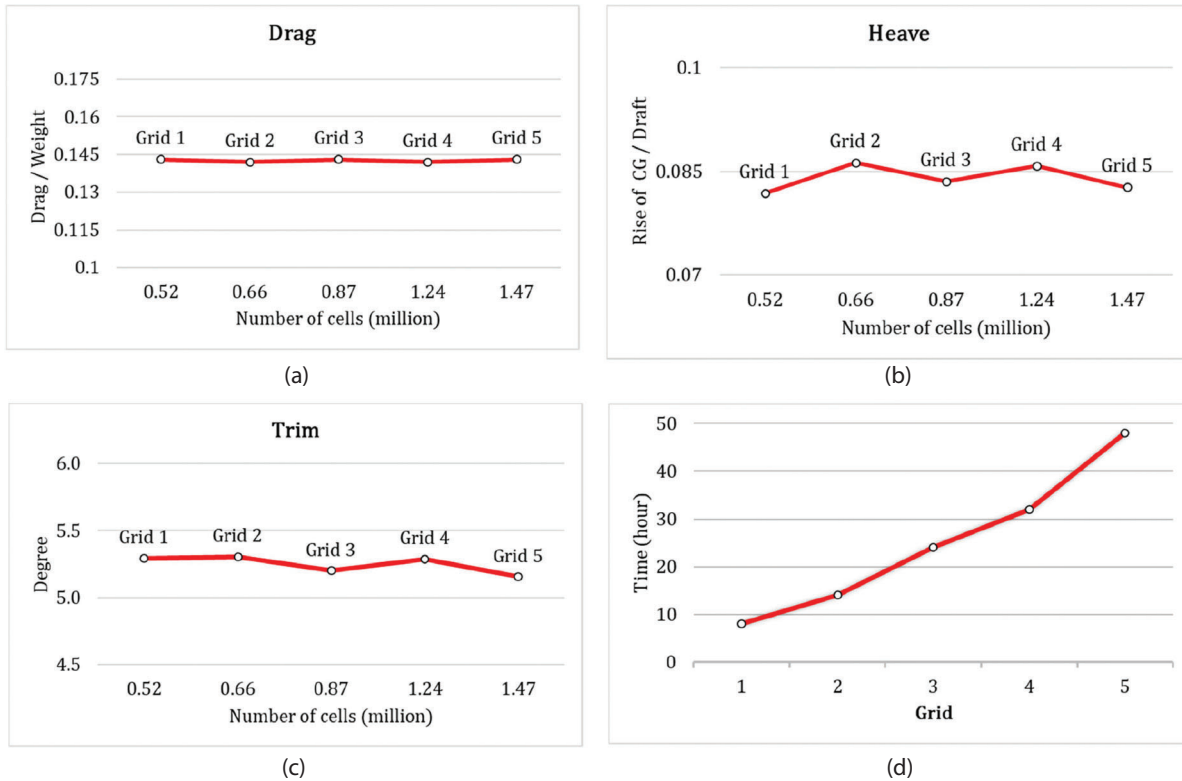


Figure 8 Grid independence study graph of (a) drag, (b) sinkage, (c) trim, (d) time
Slika 8. Grafikon analize neovisnosti mreže za (a) otpor, (b) potonuće, (c) trim, (d) vrijeme

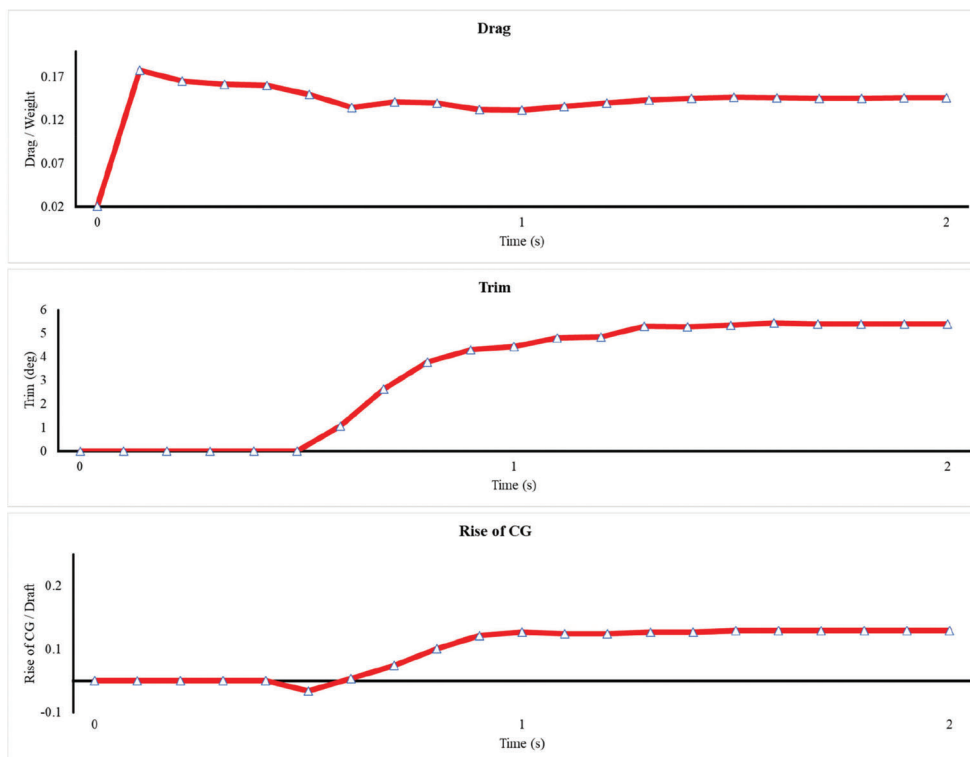
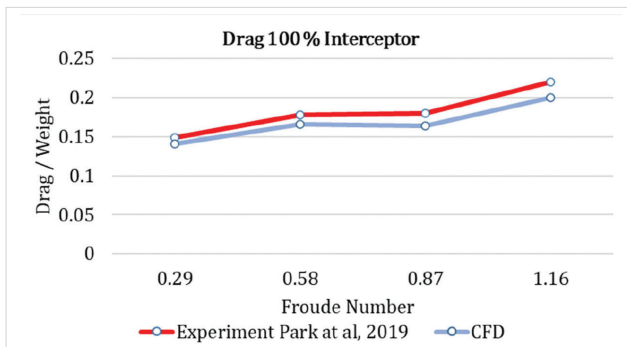


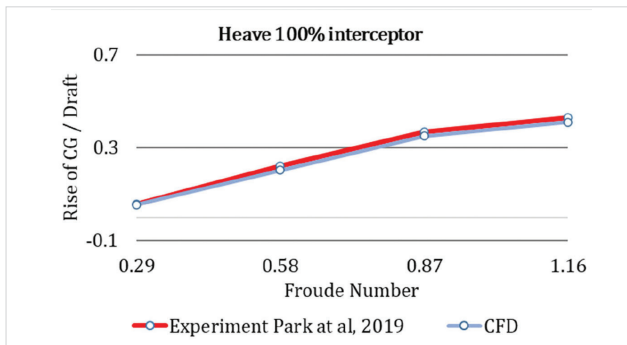
Figure 9 Convergence
Slika 9. Konvergencija

3.2. Verifying CFD and experimental results / *Provjera CFD-a i eksperimentalnih rezultata*

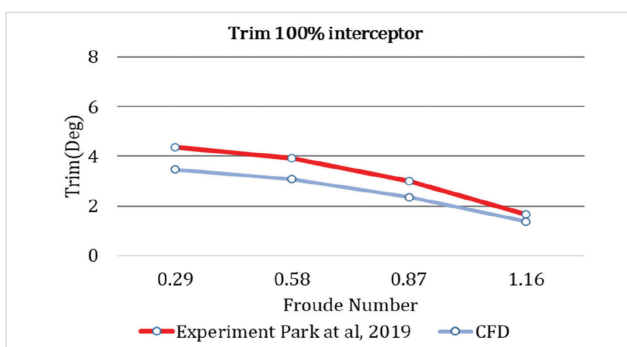
This study compares the results of the drag, sinkage, and trim analysis with 100% interceptor conditions in the close-to-keel position. Research verification by comparing the results of the CFD simulation [3] with the experimental results which can be represented in Figure 10. The graph shows the same pattern between the two research methods. Brizzola and Serra conducted a study to determine the accuracy of CFD. CFD is declared quite accurate if the maximum error tolerance is 10% [29]. Another research reported validation results more than 10% and reasonably well with the other CFD studies performed on the hull [30]. The difference between numerical and experimental ranges from 3-20% for drag and trim cases.



(a)



(b)



(c)

Figure 10 Verification of experimental result vs CFD (a) drag, (b) sinkage, (c) trim

Slika 10. Provjera eksperimentalnog rezultata u odnosu na CFD (a) otpor, (b) potonuće, (c) trim

3.3. Effect of interceptor flap variation / *Učinak varijacije zakrilca krmenog praga*

Figure 11 illustrates a comparison of the pressure variations caused by the interceptor flaps. The pressure at the bottom as measured near the hull is markedly different. As shown in Figure 11, the bottom pressure generated by the interceptor crest on the interceptor is distributed on the hull plate in front of the interceptor. The pressure produced by the interceptor flaps peaks just behind the hinge and is distributed over the interceptor flap and hull. That produces a higher pressure area than the interceptor alone (100% interceptor). This happens because the height of the interceptor is directly proportional to the resulting pressure. The high-pressure area will be higher due to the dominant interceptor as shown in Figure 12.

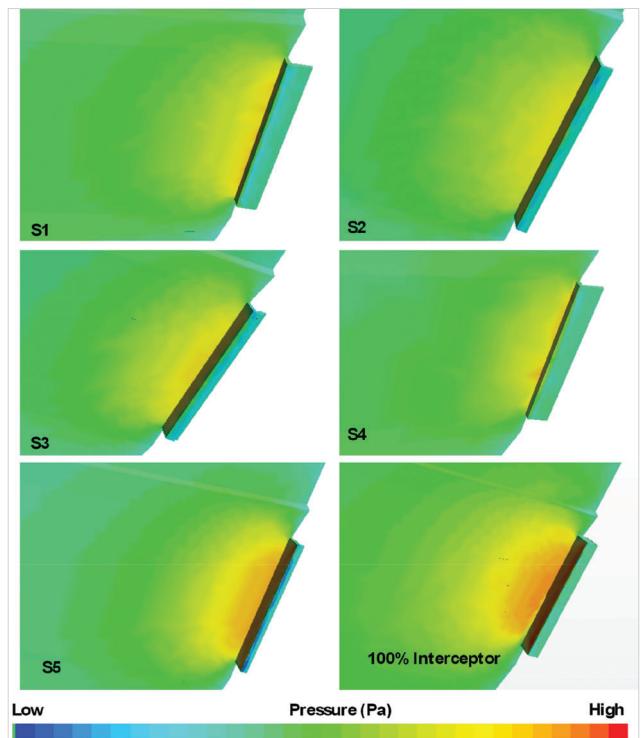


Figure 11 Pressure distribution at Froude number 1.45

Slika 11. Raspodjela tlaka pri Froudeovu broju 1,45

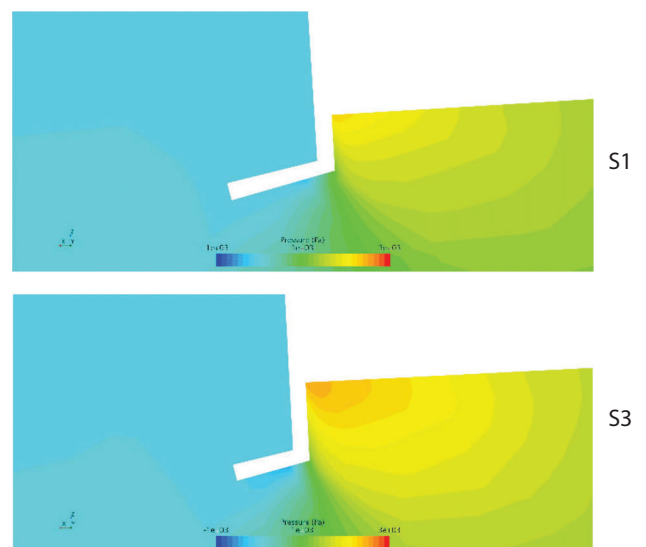


Figure 12 High pressure area created by interceptor flap

Slika 12. Područje visokog tlaka stvoreno zakrilcem krmenog praga

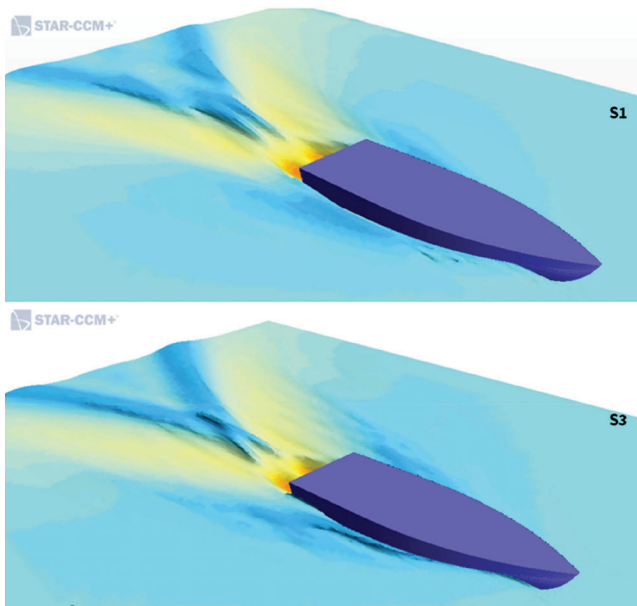


Figure 13 Wave pattern
Slika 13. Model vala

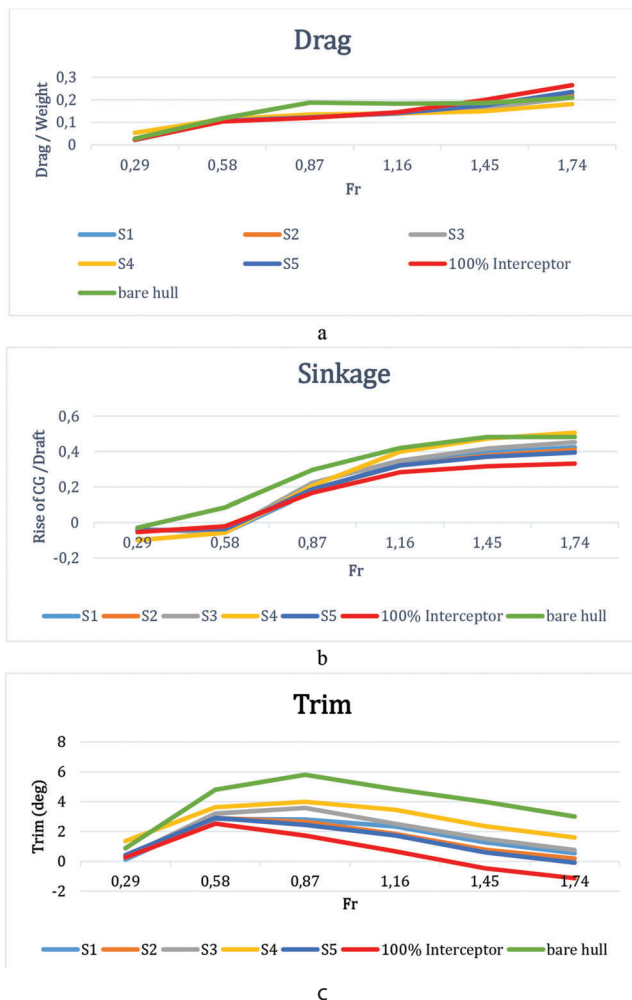


Figure 14 Result of simulation
Slika 14. Rezultat simulacije

Figure 13 describes the wave pattern between S1 and S3 at Froude number 0.87. A relatively similar pattern is produced in the figure, indicating that the modification of the flap length, which is integrated with the interceptor's height, has no significant effect.

Figure 14 shows a hydrostatic force that produced only moderately extreme ship movements visible in the displacement mode (Froude number 0.29 to 0.58). The peak position of the drag and trim values was signaled by the ship's increase in speed as it entered the transition mode (Froude number 0.87 to 1.16) of motion. This phenomenon was caused by the predominant hydrodynamic force acting upon the ship. Due to the hydrodynamic forces acting on the ship's bottom, the trim angle grew as the ship's speed did. Because the drag value under these circumstances is substantial, the interceptor was advised to be used during the transitional phase or the peak of the trim. It is not advised to use an interceptor during the planing mode period because the excessive moments the interceptor generates could cause a bow-down trim. As a result of changes in speed, the interceptor's effects on the ship's trim are a result of the ship's interaction with the interceptor. At Froude number 1.74, the ship's state revealed excessive trim, which resulted in poor ship movement. Due to too many interceptor moments, the ship experienced negative trim (bow-down trim) after the interceptor placement at a speed of 1.74. This interceptor was therefore deemed unsuitable. At Froude number 0.87, the use of an interceptor was advised to enhance the ideal trim value (fit interceptor). Each variation of the interceptor flap produces a fairly equivalent value. S5 produces the highest drag compared to other samples. The S4 produces minimum drag. The average range of using interceptor flaps to reduce drag is in the Froude number 0.29 to 1.74. The same is shown in the sinkage and trim charts. Because it is not negative, the trim value represents a safe number for all Froude ranges. The most effective drag is declared on the S4 with a reduction of 4% when compared to the 100% interceptor. In the case of 100% interceptor produces excessive drag at high speeds (Froude number >1.16). In this case, the interceptor generates a very strong moment, which may result in negative trim. Worse, this strong moment contra trim moment may cause the boat to capsize. Moreover, when S4 does not cause excessive drag or endanger the ship.

Table 3 The difference in the prediction of lift force
Tablica 3. Razlika u predviđanju sile uzgona

Variations	lift force interceptor flap (N)
S1	97.00
S2	96.76
S3	96.99
S4	96.72
S5	97.01
100% interceptor	97.01

An interceptor is a device designed to prevent the flow of water under the hull. Typically, it is a steel plate with a flat, simple design. As shown in Figure 11 it modifies the pressure distribution at the stern by forming a virtual wedge.

In Table 3, it is known that the lift force generated by each research variation is for Froude number 1.45. This research is based on CFD calculations. The greater the percentage of the interceptor height, the greater the lift force value generated. This has implications for the trim and drag moments of the ship. The interceptor is more sensitive than the flap.

The interceptor can cut the flow vertically, but the flap cuts the flow with the angle function used so that the effect of lift force, trim, and drag is less significant and less sensitive than the interceptor.

4. CONCLUSIONS / Zaključci

The object of this research is a planing hull ship with a modified interceptor installation. This study expects a reduction in drag and trim improvements that do not cause excessive pressure on the planing hull ship. The innovation of this research is the combination of the interceptor and the stern flap, hereinafter referred to as the interceptor flap. This study guarantees the accuracy of CFD by verifying the Park et al experiment. To minimize CFD inaccuracies, CFD regulation measures have followed ITTC's suggestions. The verification results show that the difference between CFD and experimental values is 3%-20% and has succeeded in showing the same pattern on the drag, sinkage, and trim comparison chart.

The use of interceptor flaps is proven to improve the performance of the planing hull ship. The lift force generated by each interceptor flap configuration shows a different effect on drag and trim. It was reported that a larger percentage of interceptors would result in a higher lift force value. A higher lift force can improve trim and reduce drag more efficiently.

This study shows a comparison between 100% interceptor and S4 variation resulting in a change in lift force of 0.3% which can have an impact on drag reduction of up to 33.3% and trim improvement of 0.8% at Froude number 1.45. It should be noted that a lift force that is too large will endanger the ship, so the design of the interceptor flap is very important in planning to make it easier to predict the lift force or ship resistance. This research is limited to the hull geometry of Aragon 2; however, different hull geometries will produce different performance levels. Nonetheless, this study is a preliminary design for a ship with an interceptor flap.

Author Contributions: Conceptualization: Samuel; Serliana Yulianti: draft preparation; Parlindungan Manik: Methodology; Andi Trimulyono: validation; Ahmad Firdhaus: Translation; Tuswan: revision; Dian Purnama Sari: revision.

Funding: The research presented in the manuscript is funded by Diponegoro University.

Conflict of interest: None of the authors have any conflicts of interest or financial ties to disclose.

Acknowledgment: The authors gratefully acknowledge financial support from Universitas Diponegoro for this work, under project scheme of "Riset Pengembangan dan Penerapan (RPP)" No. 225-08/UN7.6.1/PP/2022

REFERENCES / Literatura

- [1] Molland, A. F. (2008). A guide to ship design, construction and operation. *The Maritime Engineering Reference Book*, 636-638.
- [2] Sahin, O. S., Kahramanoglu, E., & Cakici, F. (2022). Numerical evaluation on the effects of interceptor layout and blade heights for a prismatic planing hull. *Applied Ocean Research*, 127, 1–14. <https://doi.org/10.1016/j.apor.2022.103302>
- [3] Samuel, S., Yulianti, S., Manik, P., & Fathuddiin, A. (2022). A study of interceptor performance for deep-v planing hull. *IOP Conference Series: Earth and Environmental Science*, 1081(1), 012004. <https://doi.org/10.1088/1755-1315/1081/1/012004>
- [4] Mansoori, M., & Fernandes, A. C. (2016). The interceptor hydrodynamic analysis for controlling the porpoising instability in high speed crafts. *Applied Ocean Research*, 57, 40–51. <https://doi.org/10.1016/j.apor.2016.02.006>
- [5] Karimi, M. H., Seif, M. S., & Abbaspoor, M. (2013). An experimental study of interceptor's effectiveness on hydrodynamic performance of high-speed planing crafts. *Polish Maritime Research*, 20(2), 21–29. <https://doi.org/10.2478/pomr-2013-0013>

- [6] Mansoori, M., & Fernandes, A. C. (2017). Interceptor and trim tab combination to prevent interceptor's unfit effects. *Ocean Engineering*, 134, 140–156. <https://doi.org/10.1016/j.oceaneng.2017.02.024>
- [7] Manik, P., Rindo, G., Yudo, H., & Sinaga, E. E. (2021). Analysis of the effect of addition of stern flaps on the performance of 60 m fast boat. *IOP Conference Series: Materials Science and Engineering*, 1034(1), 012032. <https://doi.org/10.1088/1757-899x/1034/1/012032>
- [8] Yaakob, O., Shamsuddin, S., & Koh, K. K. (2012). Stern Flap for Resistance Reduction of Planing Hull Craft: A Case Study with a Fast Crew Boat Model. *Jurnal Teknologi*, 41, 43–52. <https://doi.org/10.11113/jt.v41.689>
- [9] Ghadimi, P., Tavakoli, S., & Dashtimanesh, A. (2014). A Mathematical Scheme for Calculation of Lift of Planing Crafts with Large Mean Wetted Length and a Comparative Study of the Effective Parameters. *Universal Journal of Fluid Mechanics*, 2, 35–54.
- [10] Jangam, S., & Sahoo, P. (2021). Numerical investigation of interceptor effect on seakeeping behaviour of planing hull advancing in regular head waves. *Brodogradnja*, 72(2), 73–92. <https://doi.org/10.21278/brod72205>
- [11] Degiuli, N., Farkas, A., Martić, I., Zeman, I., Ruggiero, V., & Vasiljević, V. (2021). Numerical and experimental assessment of the total resistance of a yacht. *Brodogradnja*, 72(3), 61–80. <https://doi.org/10.21278/brod72305>
- [12] Tsai, J. F., & Hwang, J. L. (2005). Study on the compound effects of interceptor with stern flap for two fast monohulls. *Oceans '04 MTS/IEEE Techno-Ocean '04*, 1, 1023–1028. <https://doi.org/10.1109/oceans.2004.1405650>
- [13] Song, K. W., Guo, C. Y., Gong, J., Li, P., & Wang, L. Z. (2018). Influence of interceptors, stern flaps, and their combinations on the hydrodynamic performance of a deep-vee ship. *Ocean Engineering*, 170, 306-320. <https://doi.org/10.1016/j.oceaneng.2018.10.048>
- [14] Bondarenko, O. V., Boyko, A. P., & Zvaigzne, A. (2018). Application of the Genetic Algorithm at Initial Stages of Ships Design. *Naše More*, 65(1), 1–10. <https://doi.org/10.17818/NM/2018/1.1>
- [15] Yousefi, R., Shafaghat, R., & Shakeri, M. (2013). Hydrodynamic analysis techniques for high-speed planing hulls. *Applied Ocean Research*, 42, 105–113. <https://doi.org/10.1016/j.apor.2013.05.004>
- [16] Yulianti, S., Samuel, S., Nainggolan, T. S., & Iqbal, M. (2022). Meshing generation strategy for prediction of ship resistance using CFD approach. *IOP Conference Series: Earth and Environmental Science*, 1081(1), 012027. <https://doi.org/10.1088/1755-1315/1081/1/012027>
- [17] Sukas, O. F., Kinaci, O. K., Cakici, F., & Gokce, M. K. (2017). Hydrodynamic assessment of planing hulls using overset grids. *Applied Ocean Research*, 65, 35–46. <https://doi.org/10.1016/j.apor.2017.03.015>
- [18] Firdhaus, A., Suastika, I. K., Kiryanto, K., & Samuel, S. (2021). Benchmark Study of FINETM/Marine CFD Code for the Calculation of Ship Resistance. *Kapal: Jurnal Ilmu Pengetahuan Dan Teknologi Kelautan*, 18(2), 111–118. <https://doi.org/10.14710/kapal.v18i2.39727>
- [19] Luhulima, R. B., Sutiyo, S., & Utama, I. P. (2022). The Resistance and EEDI Analysis of Trimaran Vessel with and without Axe-bow. *Naše More*, 69(3), 132–142. <https://doi.org/10.17818/NM/2022/3.1>
- [20] Park, J.-Y., Choi, H., Lee, J., Choi, H., Woo, J., Kim, S., Kim, D. J., Kim, S. Y., & Kim, N. (2019). An experimental study on vertical motion control of a high-speed planing vessel using a controllable interceptor in waves. *Ocean Engineering*, 173, 841–850.
- [21] ITTC. (2011). *Practical Guidelines for Ship CFD Applications*.
- [22] Mansoori, M., Fernandes, A. C., & Ghassemi, H. (2017). Interceptor design for optimum trim control and minimum resistance of planing boats. *Applied Ocean Research*, 69, 100–115. <https://doi.org/10.1016/j.apor.2017.10.006>
- [23] Wilcox, D. C. (1994). Simulation of transition with a two-equation turbulence model. *AIAA Journal*, 32(2), 247–255. <https://doi.org/10.2514/3.59994>
- [24] Faltinsen, O. M. (2005). *Hydrodynamics of high-speed marine vehicles*. Cambridge university press.
- [25] Savitsky, D. (1964). Hydrodynamic design of planing hulls. *Marine Technology and SNAME News*, 1(04), 71-95.
- [26] Hosseini, A., Tavakoli, S., Dashtimanesh, A., Sahoo, P. K., & Kõrgesaar, M. (2021). Performance prediction of a hard-chine planing hull by employing different CFD models. *Journal of Marine Science and Engineering*, 9(5). <https://doi.org/10.3390/jmse9050481>.
- [27] Lotfi, P., Ashrafzaadeh, M., & Esfahan, R. K. (2015). Numerical investigation of a stepped planing hull in calm water. *Ocean Engineering*, 94, 103–110. <https://doi.org/10.1016/j.oceaneng.2014.11.022>
- [28] Avci, A. G., & Barlas, B. (2019). An experimental investigation of interceptors for a high-speed hull. *International Journal of Naval Architecture and Ocean Engineering*, 11, 256–273. <https://doi.org/10.1016/j.ijnaoe.2018.05.001>
- [29] Brizzolara, S., & Serra, F. (2007). Accuracy of CFD codes in the prediction of planing surfaces hydrodynamic characteristics. *The 2nd International Conference on Marine Research and Transportation*, 147–158. <http://www.icmrt07.unina.it/Proceedings/Papers/B/14.pdf>.
- [30] Wheeler, M. P., Matveev, K. I., & Xing, T. (2018). Validation study of compact planing hulls at pre-planing speeds. *American Society of Mechanical Engineers, Fluids Engineering Division (Publication) FEDSM*, 2, 1–8. <https://doi.org/10.1115/FEDSM2018-83091>